ISSN 1674-1056
http://cpb.iphy.ac.cn
http://iopscience.iop.org/cpb
中国物理 B
Chinese Physics
中国物理 Chinese Physics B

Growth of high quality Sr_2IrO_4 epitaxial thin films onconductive substrates

Hui Xu(徐珲), Zhangzhang Cui(崔璋璋), Xiaofang Zhai(翟晓芳), Yalin Lu(陆亚林)

Citation: Chin. Phys. B . 2019, 28(7): 078102. **doi:** 10.1088/1674-1056/28/7/078102
Journal homepage: http://cpb.iphy.ac.cn; http://iopscience.iop.org/cpb

What follows is a list of articles you may be interested in

Combinatorial synthesis and high-throughput characterization of copper-oxide superconductors

J Wu, A T Bollinger, X He, I Božović

Chin. Phys. B . 2018, 27(11): 118102. **doi:** 10.1088/1674-1056/27/11/118102

Growth of high-quality perovskite (110)-$SrIrO_3$ thin films using reactive molecular beam epitaxy

Kai-Li Zhang(张凯莉), Cong-Cong Fan(樊聪聪), Wan-Ling Liu(刘万领), Yu-Feng Wu(吴宇峰), Xiang-Le Lu(卢祥乐), Zheng-Tai Liu(刘正太), Ji-Shan Liu(刘吉山), Zhong-Hao Liu(刘中灏), Da-Wei Shen(沈大伟)

Chin. Phys. B . 2018, 27(8): 088103. **doi:** 10.1088/1674-1056/27/8/088103

Effect of substrate curvature on thickness distribution of polydimethylsiloxane thin film in spin coating process

Ying Yan(闫英), Ping Zhou(周平), Shang-Xiong Zhang(张尚雄), Xiao-Guang Guo(郭晓光), Dong-Ming Guo(郭东明)

Chin. Phys. B . 2018, 27(6): 068104. **doi:** 10.1088/1674-1056/27/6/068104

Influences of substrate temperature on microstructure and corrosion behavior of APS $Ni_{50}Ti_{25}Al_{25}$ inter-metallic coating

Sh Khandanjou, M Ghoranneviss, Sh Saviz, M Reza Afshar

Chin. Phys. B . 2018, 27(2): 028104. **doi:** 10.1088/1674-1056/27/2/028104

Preparation and characterization of PTFE coating in new polymer quartz piezoelectric crystal sensor for testing liquor products

Gu Yu, Li Qiang

Chin. Phys. B . 2015, 24(7): 078106. **doi:** 10.1088/1674-1056/24/7/078106

Growth of high quality Sr_2IrO_4 epitaxial thin films on conductive substrates*

Hui Xu(徐珲)[1], Zhangzhang Cui(崔璋璋)[1,2], Xiaofang Zhai(翟晓芳)[1,3,†], and Yalin Lu(陆亚林)[1,2,4,‡]

[1] *Hefei National Laboratory for Physical Sciences at the Microscale, University of Science and Technology of China, Hefei* 230026, *China*
[2] *National Synchrotron Radiation Laboratory, University of Science and Technology of China, Hefei* 230026, *China*
[3] *Synergy Innovation Center of Quantum Information and Quantum Physics, University of Science and Technology of China, Hefei* 230026, *China*
[4] *Department of Materials Science and Engineering, University of Science and Technology of China, Hefei* 230026, *China*

(Received 18 February 2019; revised manuscript received 1 April 2019; published online 31 May 2019)

Ruddlesden–Popper iridium oxides have attracted considerable interest because of the many proposed novel quantum states that arise from the large spin–orbit coupling of the heavy iridium atoms in them. A prominent example is the single layer Sr_2IrO_4, in which superconductivity has been proposed under electron doping. However, the synthesis of Sr_2IrO_4 high quality thin films has been a huge challenge due to the easy formation of impurities associated with different numbers of SrO layers. Thus techniques to optimize the growth of pure phase Sr_2IrO_4 are urgently required. Here we report the deposition of high quality Sr_2IrO_4 thin films on both insulating $SrTiO_3$ and conducting $SrTiO_3$:Nb substrates using pulsed laser deposition assisted with reflective high-energy electron diffraction. The optimal deposition temperature of Sr_2IrO_4 epitaxial films on $SrTiO_3$:Nb substrates is about 90 °C lower than that on $SrTiO_3$ substrates. The electrical transports of high quality Sr_2IrO_4 films are measured, which follow the three-dimensional Mott variable-range hopping model. The film magnetizations are measured, which show weak ferromagnetism below ~ 240 K with a saturation magnetization of $\sim 0.2\ \mu_B$/Ir at 5 K. This study provides applicable methods to prepare high quality 5d Sr_2IrO_4 epitaxial films, which could be extended to other Ruddlesden–Popper phases and potentially help the future study of exotic quantum phenomena in them.

Keywords: substrates, pulsed laser deposition, iridates, conduction mechanism

PACS: 81.15.–z, 61.05.jh, 71.70.Ej, 71.27.+a **DOI:** 10.1088/1674-1056/28/7/078102

1. Introduction

In recent years, the Ruddlesden–Popper iridium oxides $Sr_{n+1}Ir_nO_{3n+1}$ ($n = 1, 2, \ldots$) have attracted broad interest because of their novel quantum ground states, which arise from the large spin–orbit coupling of the heavy iridium element ($Z = 77$).[1–3] The $n = 1$ Sr_2IrO_4 is a representative spin–orbit-coupled Mott insulator with $J_{\rm eff} = 1/2$.[4] Due to the competition between the strong spin–orbit coupling and Coulomb repulsion (~ 0.5 eV), a narrow gap is formed between the half-filled and half-empty $J_{\rm eff} = 1/2$ bands.[2,5,6] The electrical properties and lattice structure of Sr_2IrO_4 are both similar to those of the parent compound of high-temperature superconducting cuprate La_2CuO_4.[6,7] Previous theoretical studies suggest the possibility of unconventional superconductivity in electron doped Sr_2IrO_4.[8,9] To study the physical properties and perhaps to reveal exotic phenomena such as unconventional superconductivity, techniques to fabricate high-quality single-crystalline Sr_2IrO_4 thin films are in urgent need.[10] Pulsed laser deposition (PLD) assisted with reflective high-energy electron diffraction (RHEED) is a typical physical vapor-deposition technique that has been widely used to prepare high quality complex oxide thin films.[11–13] One can accurately control the composition of the thin films via PLD.[5] Though the growth of simple orthorhombic $SrIrO_3$ films is relatively straight-forward, only a handful of groups reported the successful growth of Sr_2IrO_4 single-crystalline films.[2,10,14] The Sr_2IrO_4 films usually contain various impurity phases such as $SrIrO_3$ and $Sr_3Ir_2O_7$, and have poor crystalline structures even with a stoichiometric Sr_2IrO_4 target.[5,10] Besides, very high growth temperatures are usually needed to prepare Sr_2IrO_4 films.[14] Unfortunately, the high growth temperature may exceed the temperature range of the heating plate of the PLD chamber and long-term experiments at those temperatures may damage the heating plate. Therefore, the capability to grow high quality epitaxial Sr_2IrO_4 thin films at lower temperatures is urgent required. According to previous works, an important method to prepare high-quality layered-perovskite films is to reduce the interface energy between the substrates and deposited films.[15–17] At present, the commonly used method to reduce the interface energy is to grow a conductive layer; i.e., a high-quality buffer layer between the films and substrates.[15] Whereas, the insertion of buffer layers can cause new problems such as ion-diffusion between the film

*Project supported by the National Natural Science Foundation of China (Grant Nos. 51627901 and 11574287), the National Key Research and Development Program of China (Grant No. 2016YFA0401004), and Hefei Science Center-Chinese Academy of Sciences (Grant No. 2016HSC-IU004). X. Z. acknowledges the support of the Youth Innovation Promotion Association of Chinese Academy of Sciences (Grant No. 2016389).

†Corresponding author. E-mail: xfzhai@ustc.edu.cn
‡Corresponding author. E-mail: yllu@ustc.edu.cn

© 2019 Chinese Physical Society and IOP Publishing Ltd

and buffer layers that can lead to the formation of impurities at high temperatures.

In our study, we find that the optimal growth temperature for epitaxial Sr_2IrO_4 films on $SrTiO_3$:Nb (001) conductive substrates is ~ 90 °C lower than that on insulating $SrTiO_3$ (001) substrates using PLD assisted with RHEED. Electrical transport measurements of the Sr_2IrO_4 films on $SrTiO_3$:Nb substrates are performed, which show a three-dimensional Mott variable-range hopping mechanism, and the films exhibit weak ferromagnetism below ~ 240 K with a saturation magnetization of ~ 0.2 μ_B/Ir at 5 K. Both the above electrical transport and magnetization characters match those of the high quality Sr_2IrO_4 films grown on insulating $SrTiO_3$ substrates at the higher temperature. This study demonstrates that conductive substrates reduce the optimal growth temperature for preparing high quality Sr_2IrO_4 thin films, which may facilitate future studies of exotic phenomena in the Sr_2IrO_4 family.

2. Experiment

The Sr_2IrO_4 thin films (with thickness of about 25 nm) were grown on (001) oriented $SrTiO_3$ and $SrTiO_3$: 0.7%wt. Nb single-crystalline substrates using PLD assisted with RHEED. A commercial stoichiometric Sr_2IrO_4 target was used for all film growths in this study. The background pressure of the PLD chamber was about 10^{-6} Pa. A KrF exciter laser ($\lambda = 248$ nm) was used with different fluence energies at the frequency of 1 Hz. During the deposition, oxygen pressures between 0.01 Pa to 20 Pa and substrate temperatures ranging from 670 °C to 870 °C for $SrTiO_3$:Nb and 770 °C to 860 °C for $SrTiO_3$ were used. A high-quality $LaNiO_3$ buffer layer of 40 nm was deposited at 660 °C and 30 Pa to make a comparison with the growth directly on $SrTiO_3$:Nb substrates.[15] The actual growth temperatures were measured using an external infrared detector for every deposition condition. The possibility of the observed temperature difference being from different emissivities was rule out using Au/Ti back-coated $SrTiO_3$ substrates and simultaneous heating of both insulating and conductive substrates. X-ray diffraction (XRD) characterization was performed using a Rigaku SmartLab high-resolution diffractometer with wavelength of 0.15406 nm from Cu $K\alpha$ radiation. The I–V measurements were done using the 4-wire method with Ti/Au top electrodes. The magnetic and electrical properties of the Sr_2IrO_4 films were characterized by a Quantum Design physical property measurement system.

3. Results and discussion

Figure 1(a) displays the XRD patterns of the Sr_2IrO_4 films grown on insulating $SrTiO_3$ substrates with an energy density of 0.5 J/cm^2 and oxygen pressures of 0.2 Pa and 0.4 Pa, respectively. All diffraction peaks of the film grown at 850 °C can be indexed to the (0 0 L) reflections of the Sr_2IrO_4 single crystal (see Fig. 1(a)), thus indicating the Ruddlesden–Popper $n = 1$ crystal structure. In addition, there are no impurity phase related peaks. The film thickness oscillation is observed, which suggests the film interface and surface being very smooth. The c-axis lattice constant of the film is about 2.5072 nm. When the growth temperature is 800 °C, the (0 0 L) diffraction peaks of the Sr_2IrO_4 film are weak and even the (0 0 8) peaks are almost invisible, which can be summarized as phase II range in Fig. 1(c). An extra peak at $2\theta = 20.92°$ (marked with a red star) appears, which matches very well with the (0 0 1) diffraction of the $SrIrO_3$ phase. As the deposition temperature is decreased below 700 °C, the diffraction peaks of $SrIrO_3$ with much smaller c-axis lattice constant appear at $2\theta = 21.8°$ and 44.3°. The $SrIrO_3$ phase is very stable and no Sr_2IrO_4 phase is observed. This corresponds to phase I in Fig. 1(c). Unfortunately, the heating temperature of our PLD instrument cannot be higher than 870 °C. Therefore, figure 1(c) shows no XRD data of samples on insulating substrates with higher growth temperatures in the phase IV region.

Figure 1(b) shows that the optimized deposition temperature of Sr_2IrO_4 films on $SrTiO_3$:Nb conductive substrates is about 780 °C. Both (0 0 12) peaks of the Sr_2IrO_4 samples on $SrTiO_3$ and $SrTiO_3$:Nb substrates are at 42.2° ($c = 2.572$ nm). The film in phase IV, which was grown at 840 °C, exhibits the impurity phases of iridium and $SrIrO_3$. The inconspicuous

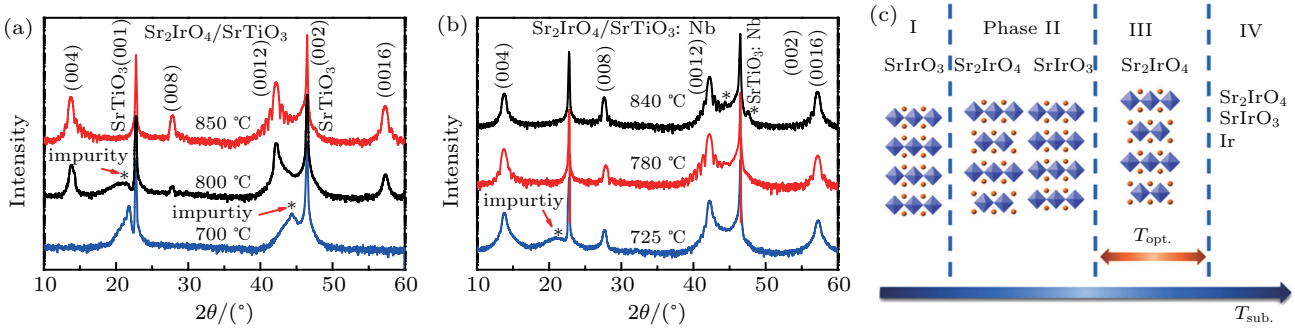


Fig. 1. The XRD patterns of (a) $Sr_2IrO_4/SrTiO_3$ (001) films and (b) $Sr_2IrO_4/SrTiO_3$: Nb (001) samples grown at different substrate temperatures. The black stars mark the impurity phase peaks. (c) Temperature dependence of the structure of different SrO layer number phases. Temperatures in the phase III range indicate the substrate temperature for Sr_2IrO_4 epitaxial film growth.

appearance of an extra peak at $2\theta = 44.4°$ matches very well with the (0 0 2) diffraction of the $SrIrO_3$ phase in Fig. 1(b). The XRD pattern of the film deposited at 725 °C shows poor crystallinity of the Sr_2IrO_4 phase and a clear perovskite peak of $SrIrO_3$ without film-thickness oscillation in phase II. It is remarkable that the optimal deposition temperature of the Sr_2IrO_4 films on $SrTiO_3$:Nb conductive substrates is about 90 °C lower than that directly deposited on insulating $SrTiO_3$ substrates. The Sr_2IrO_4 films are coherently strained to the substrates, as confirmed by the x-ray reciprocal space mapping measurements and RHEED patterns obtained before and after the deposition. Therefore, the substrate induced strain cannot explain the large drop of the optimal deposition temperatures. The sharp drop in the growth temperature of Sr_2IrO_4 films on conductive substrates may suggest that the interface between the Sr_2IrO_4 film and $SrTiO_3$:Nb substrate has a much smaller interface energy than that between Sr_2IrO_4 and the $SrTiO_3$ insulating substrate.

To elucidate the specific phase compositions of the films, the samples deposited at diverse substrate temperatures are separated into I, II, III, and IV regions in Fig. 1(c), where the horizontal axis represents the substrate temperature and the vertical axis represents the oxygen pressure. Figure 1(c) also shows the crystal structure of $SrIrO_3$ as a major impurity in addition to the Sr_2IrO_4 main phase. Below the optimal temperature range (phases I and II), the films exhibit either a single $SrIrO_3$ phase or a Sr_2IrO_4 phase with $SrIrO_3$ impurities. There is a wide window for the stabilization of pseudo-cubic $SrIrO_3$ phase for all P_{O_2} grown at substrate temperatures below 740 °C. In the region of phase III, a single Sr_2IrO_4 phase with good crystallinity is found. Above this range (i.e., in phase IV), the films exhibit a layered Sr_2IrO_4 phase and impurity phases of $SrIrO_3$ and metallic iridium. This may indicate that the layered Sr_2IrO_4 films are partially converted to the perovskite $SrIrO_3$. During exploring the substrate temperature dependence for Sr_2IrO_4 films on both types of substrates, the oxygen pressure was also optimized in a range between 0.01 Pa and 20 Pa. Therefore, our results indicate that the optimal deposition temperature for Sr_2IrO_4 films on $SrTiO_3$:Nb conductive substrates is approximately 90 °C lower than that grown on $SrTiO_3$ substrates.

To further confirm the results, Sr_2IrO_4 epitaxial films were grown on $SrTiO_3$ substrates with $LaNiO_3$ buffer layers as well as on $SrTiO_3$ substrates with Ti (50 nm) or Au (50 nm) layers sequentially sputtered on the back. The RHEED was used to monitor the *in-situ* layer-by-layer epitaxial growth or three-dimensional islands-growth of the thin films at low oxygen pressure. The typical XRD patterns of the Sr_2IrO_4 films grown on different substrates under optimal conditions are shown in Fig. 2(a). The sharp (0 0 L) diffraction peaks of the Sr_2IrO_4 films suggest that the samples are of high crystallinity, and there are no observable impurities, such as $SrIrO_3$. Figure 2(b) shows the intensity oscillations of RHEED for Sr_2IrO_4 samples deposited on diverse substrates. The reflected beam-intensity oscillations, with a certain intensity for the films deposited on conductive substrate $SrTiO_3$:Nb or $LaNiO_3$ buffer layer, demonstrate a two-dimensional layer-by-layer growth mode. The growth temperature for the Sr_2IrO_4 films on $SrTiO_3$ substrates with the $LaNiO_3$ buffer layer is also reduced by nearly 40 °C compared to that directly grown on $SrTiO_3$ substrates. On the other hand, the optimal temperature on the $SrTiO_3$ substrates with Ti and Au metal sputtered on the back is not significantly reduced compared with that of the films grown on bare $SrTiO_3$. Therefore, the possibility that the decrease of growth temperature on $SrTiO_3$:Nb due to impurities at the substrate and film interface may be ruled out. Thus, it is speculated that the interface energy between the Sr_2IrO_4 films and $SrTiO_3$:Nb conductive substrates is reduced similar to the interface energy decrease between the Sr_2IrO_4 films and $LaNiO_3$ buffer layers. In a previous study, our group has achieved great enhancement of crystalline quality of Aurivillius films by applying a conductive $LaNiO_3$ buffer layer to screen the electric dipole field in the film. However, the $Sr_2IrO_4/SrTiO_3$:Nb interface does not exhibit the polar catastrophe as in previous Aurivillius films and the mechanism might be different.[15] A simple model is used to explain the difference in optimal growth temperatures on different substrates. When the atoms arrive at the substrate, they are adsorbed by the surface to form a stable phase of the oxide. So far, this adsorption is a physical adsorption and not a chemical bond. To form a heterostructure, these atoms need to overcome an energy barrier to position at the correct place for forming a stable chemical bond, mostly by thermal diffusion. One possible explanation for the reduced optimal growth temperature is that the bonding energy of Sr_2IrO_4 on $SrTiO_3$:Nb is much lower than that of Sr_2IrO_4 on $SrTiO_3$.

Figures 3(a) and 3(b) show that the growth of Sr_2IrO_4 films is affected by the oxygen pressure (P) and the deposition temperature (T) on both $SrTiO_3$:Nb (see Fig. 3(a)) and $SrTiO_3$ substrates (see Fig. 3(b)). A large number of samples were grown at oxygen pressures ranging from 0.01 Pa to 20 Pa and deposition temperatures from 670 °C to 830 °C on $SrTiO_3$:Nb and from 770 °C to 860 °C on $SrTiO_3$. The different patterns represent different identified phases in the films for different growth conditions. Figure 3(b) shows that the deposition-condition range for Sr_2IrO_4 films grown on $SrTiO_3$ (001) substrates is very narrow, and the temperature needs to exceed 840 °C. It is clear that high-quality Sr_2IrO_4 ($n = 1$) films on conductive $SrTiO_3$:Nb substrates have lower growth temperatures as well as a wider window for the substrate temperature (ranging from 750 °C to high temperatures shown in Fig. 3(a)). By comparing the two figures, the growth temperature for Sr_2IrO_4 thin films on $SrTiO_3$:Nb substrates is about 90 °C lower than that directly grown on $SrTiO_3$ sub-

strates. To explain the phase diagram, the laser plume is assumed to contain multiple substances, such as SrO, IrO_3, $SrIrO_3$, Sr_2IrO_4, IrO_2, IrO_6, etc. As the oxygen pressure increases, a pure $SrIrO_3$ film is obtained. If a large amount of $SrIrO_3$ is contained in the plume when the oxygen pressure increases, then the reaction $2SrIrO_3 + O_2 = 2Sr_2IrO_4 + 2IrO_3$ will generate more Sr_2IrO_4.[1] As it is not the case, this possibility can be excluded. However, it can explain why $SrIrO_3$ is also produced under the low oxygen pressure. The high oxygen pressure leads to the pure phase $SrIrO_3$ via the reactions $Sr_2IrO_4 + Ir + O_2 = 2SrIrO_3$ and $2Sr_2IrO_4 + 2IrO_3 = 4SrIrO_3 + O_2$, where Ir may be derived from enriched Ir in the target.[10] According to the literature, IrO_3 is a stable gaseous compound, and is more stable than IrO_2, which therefore excludes IrO_2 as the main component of the plume. Another explanation is that the lighter SrO species is likely to be backscattered by oxygen atoms under high oxygen pressure. Recent studies found that the light species SrO has a wider distribution than the heavy species at a high oxygen pressure, according to the x-ray photoelectron spectroscopy measurement. Hence, the epitaxial films have an Ir rich formation like $SrIrO_3$.[5]

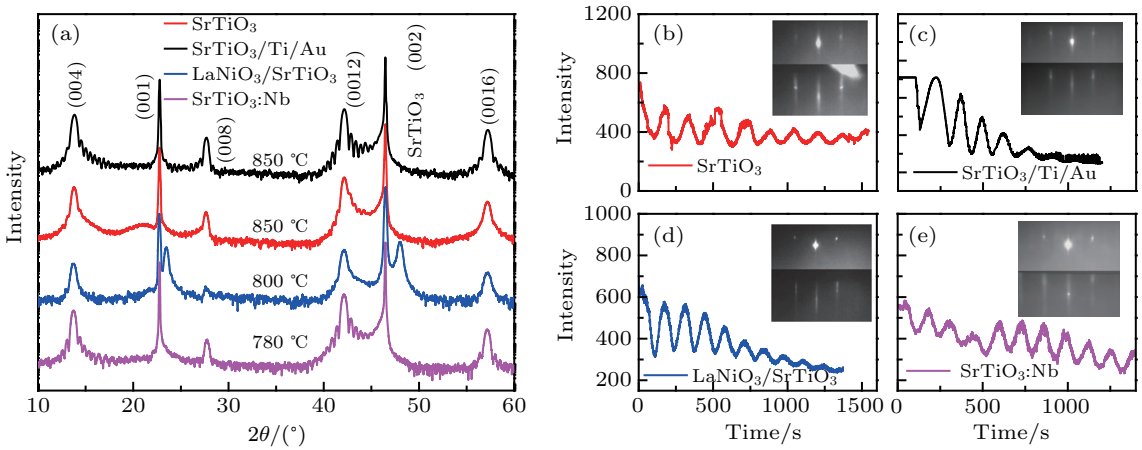


Fig. 2. (a) XRD patterns of Sr_2IrO_4 samples grown on different substrates. (b)–(e) RHEED intensity oscillations for Sr_2IrO_4 films grown under optimization condition on (b) (001)-oriented $SrTiO_3$ substrate without buffer layer, (c) $SrTiO_3$ substrates with titanium and gold sequentially sputtered on the back of the substrates, (d) $SrTiO_3$ substrate with buffer layer $LaNiO_3$, (e) $SrTiO_3$:Nb substrate.

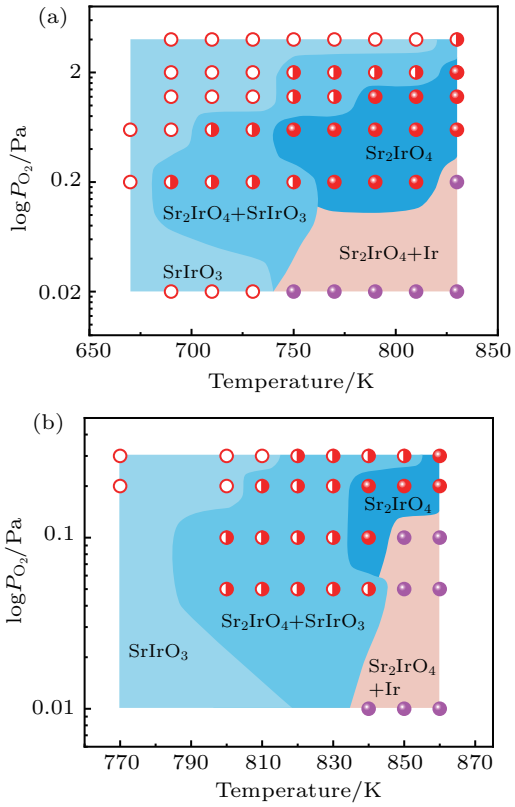


Fig. 3. The phase diagram of Sr_2IrO_4 grown on (a) $SrTiO_3$:Nb and (b) $SrTiO_3$ substrates.

Figure 4(a) displays that the full-width at half-maximum of the (0 0 12) rocking curve is 0.04° for the Sr_2IrO_4 films on $SrTiO_3$:Nb (001), consistent with phase III in Fig. 1(c). The inset of Fig. 4(b) shows the resistivity as a function of temperature between 50 K and 360 K for the high-quality Sr_2IrO_4 samples grown on $SrTiO_3$ and $SrTiO_3$:Nb (001) substrates, respectively. The conduction mechanism responsible for the electrical transport in Sr_2IrO_4 films is illustrated in Fig. 4(b).[2] In Fig. 4(b), the illustration of $\ln\rho$ versus $T^{-1/4}$ for the Sr_2IrO_4 films shows two temperature ranges. The three-dimensional Mott variable-range hopping mechanism is used to explain the transport characteristics of the Sr_2IrO_4 film. The values of T_M, the average hopping distance R_M, the localization length a, and the Mott hopping energy of the sample on an insulating substrate were calculated.[2] The corresponding results are listed in Table 1. By comparison, the resistivity ρ of the film on insulating substrate is slightly higher. While the sample on insulating substrate also shows insulating behavior and two temperature ranges with good linear relationship of $\ln\rho$–$T^{-1/4}$, which are consistent with the film on conductive substrate. The zero-field cooling and field cooling magnetization results for the film grown on $SrTiO_3$:Nb (001) are shown in Fig. 4(c). The transition temperature T_C of the weak ferromagnetism is about 240 K and the saturation magnetization is $\sim 0.2\ \mu_B$/Ir (see inset in Fig. 4(c)).

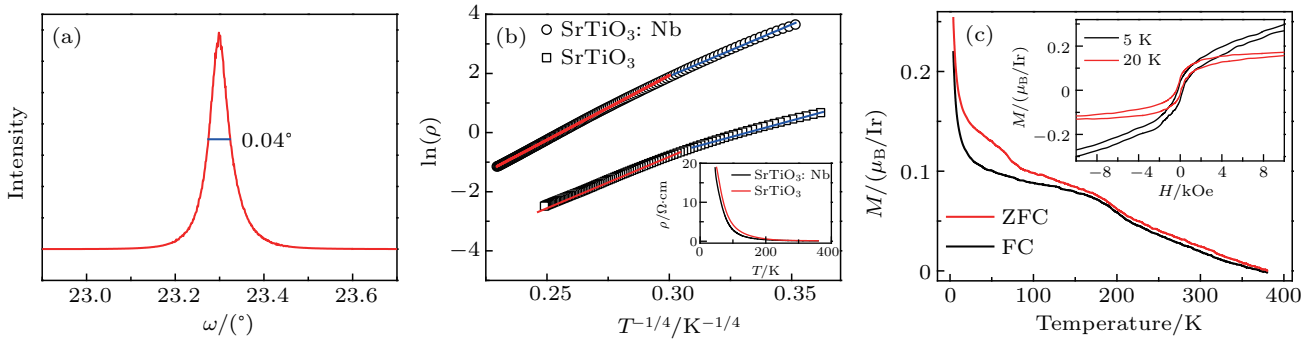


Fig. 4. (a) The crystal quality of epitaxial Sr_2IrO_4 film on $SrTiO_3$:Nb (001) is shown by the full-width at half-maximum of (0 0 12) x-ray rocking curve. (b) Temperature dependence of the resistivity of Sr_2IrO_4 epitaxial films on $SrTiO_3$ and $SrTiO_3$:Nb substrates, the inset shows $\ln\rho$ versus $T^{-1/4}$. (c) The field cool and zero-field cool curves and the inset shows the hysteresis loops of epitaxial Sr_2IrO_4 film at 5 K and 20 K, respectively.

Table 1. Fitting parameters to the three-dimensional Mott variable range hopping model for Sr_2IrO_4 thin film on $SrTiO_3$ substrate.

Temperature	$T_M/10^6$ K	a/Å	$(R_M/a)/K^{-1/4}$	E_M/meV
High-T	1.5	1.9	$12.9/T^{1/4}$	$0.71/T^{3/4}$
Low-T	0.6	2.6	$10.1/T^{3/4}$	$0.58/T^{3/4}$

4. Conclusion

We have grown high-quality Sr_2IrO_4 thin films on both conductive $SrTiO_3$:Nb and insulating $SrTiO_3$ substrates using PLD assisted with RHEED. The results indicate that the suitable growth temperature for Sr_2IrO_4 films on $SrTiO_3$:Nb substrate is at least 90 °C lower than that on $SrTiO_3$, suggesting that the interface energy barrier between the Sr_2IrO_4 films and $SrTiO_3$:Nb substrates is lower than that between Sr_2IrO_4 and the $SrTiO_3$ substrates. The electrical transport of high-quality Sr_2IrO_4 films grown on $SrTiO_3$ substrates is discussed, which agrees to the three-dimensional Mott variable-range hopping conduction rule. The magnetization measurements show that the films exhibit weak ferromagnetism with T_C of about 240 K and the saturation magnetization of ~ 0.2 μ_B/Ir at 5 K. The study proves the crucial role of conductive substrates (such as $SrTiO_3$:Nb) to reduce the optimal growth temperature in depositing high-quality iridium oxide thin films.

References

[1] Nishio K, Hwang H Y and Hikita Y 2016 *APL Mater.* **4** 036102

[2] Lu C L, Quindeau A, Deniz H, Preziosi D, Hesse D and Alexe M 2014 *Appl. Phys. Lett.* **105** 082407

[3] Zhang K L, Fan C C, Liu W L, Wu Y F, Lu X L, Liu Z T, Liu J S, Liu Z H and Shen D W 2018 *Chin. Phys. B* **27** 088103

[4] Nichols J, Terzic J, Bittle E G, Korneta O B, De Long L E, Brill J W, Cao G and Seo S S A 2013 *Appl. Phys. Lett.* **102** 141908

[5] Liu X R, Cao Y W, Pal B, Middey S, Kareev M, Choi Y, Shafer P, Haskel D, Arenholz E and Chakhalian J 2017 *Phys. Rev. Mater.* **1** 075004

[6] Kim B J, Moon S J, Kim J Y, Park B G, Leem C S, Yu J, Noh T W, Kim C, Oh S J, Park J H, Durairaj V, Cao G and Rotenberg E 2008 *Phys. Rev. Lett.* **101** 076402

[7] Cao G, Bolivar J, Mccall S, Crow J E and Guertin R P 1998 *Phys. Rev. B* **57** R11039

[8] Mitchell J F 2015 *APL Mater.* **3** 062404

[9] Watanabe H, Shirakawa T and Yunoki S 2013 *Phys. Rev. Lett.* **110** 027002

[10] Chen B J, Yang N, Zhong N, Tang X D, Yang P X, Xiang P H and Duan C G 2017 *Mater. Lett.* **202** 96

[11] Meng D C, Zhai X F, Ma C, Huang H L, Yun Y, Huang Y, Fu Z P, Peng R R, Mao X Y, Chen X B, Brown G and Lu Y L 2015 *Appl. Phys. Lett.* **106** 212906

[12] Yun Y, Zhai X F, Ma C, Huang H L, Meng D C, Cui Z Z, Wang J L, Fu Z P, Peng R R, Brown G J and Lu Y L 2015 *Appl. Phys. Express* **8** 054001

[13] Cui Z Z, Xu H, Yun Y, Guo J H, Chuang Y D, Huang H L, Meng D C, Wang J L, Fu Z P, Peng R R, Knize R J, Brown G J, Zhai X F and Lu Y L 2016 *J. Appl. Phys.* **120** 084101

[14] Serrao C R, Liu J, Heron J T, Singh-Bhalla G, Yadav A, Suresha S J, Paull R J, Yi D, Chu J H , Trassin M, Vishwanath A, Arenholz E, Frontera C, Zelezny J, Jungwirth T, Marti X and Ramesh R 2013 *Phys. Rev. B* **87** 085121

[15] Yun Y, Ma C, Zhai X F, Huang H L, Meng D C, Wang J L, Fu Z P, Peng R R, Brown G J and Lu Y L 2015 *Appl. Phys. Lett.* **107** 011602

[16] Lee J H, Luo G, Tung I C, Chang S H, Luo Z, Malshe M, Gadre M, Bhattacharya A, Nakhmanson S M, Eastman J A, Hong H, Jellinek J, Morgan D, Fong D D and Freel J W 2014 *Nat. Mater.* **13** 879

[17] Zheng H M, Zhan Q, Zavaliche F, Sherburne M, Straub F, Cruz M P, Chen L Q, Dahmen U and Ramesh R 2006 *Nano Lett.* **6** 1401